

Optimal Routing and Energy Management Strategies for Plug-in Hybrid Electric Vehicles

Mauro Salazar¹, Arian Houshmand², Christos G. Cassandras² and Marco Pavone¹

Abstract— This paper presents eco-routing strategies for plug-in hybrid electric vehicles, whereby we jointly compute the routing and energy management strategy and the objective is a combination of travel time and energy consumption. Specifically, we first use Pontryagin’s principle to compute the optimal Pareto front in terms of achievable fuel and battery consumption for different types of road links. Second, we leverage these Pareto fronts to formulate a network flow optimization problem to compute the optimal routing and energy management strategy, minimizing a combination of travel time and energy consumption. Finally, we present a real-world case-study for the Eastern Massachusetts highway sub-network. The proposed approach allows to compute the optimal solution for different objectives, ranging from minimum time to minimum energy, revealing that by sacrificing a small amount of travel time significant improvements in fuel consumption can be achieved.

I. INTRODUCTION

HYBRID electric vehicles (HEVs) are emerging on the market as a short-term solution to improve the fuel economy and reduce the environmental impact of a wide range of vehicles. Compared to pure internal combustion engine (ICE) vehicles, they can achieve significant reductions in fuel consumption and emissions by recuperating braking energy and operating the engine in a more efficient fashion through load-point shifting [1]. Compared to electric vehicles, HEVs have a significantly larger range, due to the high energy density of fuels compared to today’s batteries. Moreover, the refueling process is achieved in a couple of minutes, whereas it usually takes hours to recharge a battery. Plug-in HEVs feature the additional possibility to directly recharge the battery, therefore allowing for a fully-electric driving mode. In fact, depending on their battery size, they can be driven 20–70 km in fully-electric mode, which corresponds to the average daily commuting distance in the US [2]. Nevertheless, to fully exploit the potential of HEVs, the energy management system coordinating the energy flows among the powertrain components needs to be carefully designed. Specifically, the power split between the engine and the electric machine is controlled to minimize fuel consumption whilst meeting a predefined battery charge target at the end of the driving mission. Conventional HEVs are usually in battery-charge-sustaining mode, whilst plug-in HEVs also allow battery-discharging modes, for instance through fully-electric driving, as they can then be recharged like conventional electric vehicles. To this end, predictive information on the optimal battery energy trajectory to be followed during the driving mission can provide significant

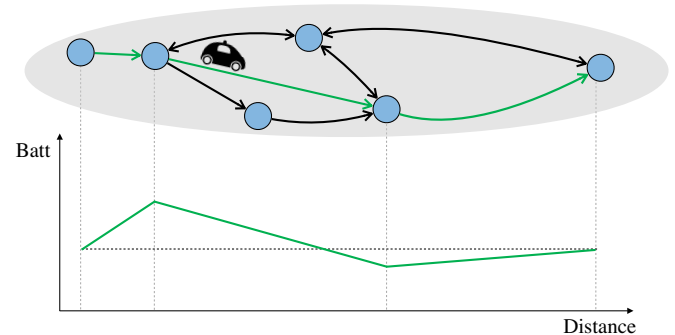


Fig. 1. Road digraph with blue dots representing intersections and arcs denoting road-links (black). In green the optimal eco-route is shown together with the optimal battery energy trajectory.

additional benefits with respect to reactive strategies. The possibility of also controlling the speed profile (as with adaptive cruise controllers or autonomous vehicles) or the vehicle route offer further margins to improve the fuel economy of the HEV.

In this paper, we study the possibility of jointly computing the optimal routing and energy management strategies minimizing a combination of travel time and energy consumption, thus providing the route to be followed and the battery charge trajectory to be tracked by the energy management system, as shown in Fig. 1.

Literature Review: The work presented in this paper contributes to two streams of research, namely high-level energy management of hybrid electric powertrains and vehicle routing. In the following, we review these two streams in turn.

The fuel-optimal control of HEVs is divided into non-causal optimization methods for the strategic analysis of perfectly known driving cycles and real-time control applications. Non-causal control approaches (i.e., where the driving mission is assumed to be known *a priori*) are based on dynamic programming [3], [4], convex optimization [5]–[7] and Pontryagin’s minimum principle (PMP) [8]–[10], whilst real-time algorithms rely on rule-based strategies [11], [12], on equivalent consumption minimization strategies (ECMS) [13], [14], and model predictive control [15]–[17]. Such approaches are based on the assumption that the route is predefined and cannot be optimized. However, state-of-the-art control algorithms rely on predictive route information, such as an expected driving cycle or an optimal battery energy trajectory to track, since it can significantly improve the overall performance [18].

Traditional vehicle routing algorithms try to find the fastest or shortest path routes [19], [20], whereas eco-routing algorithms seek to find the routes that minimize the energy consumption costs. For conventional ICE vehicles there are

¹Autonomous Systems Lab, Stanford University, United States {samauro, pavone}@stanford.edu

² Division of Systems Engineering, Boston University, United States {arianh, cgc}@bu.edu

already many eco-routing algorithms available capable of finding the energy-optimal paths based on historical and real-time traffic data [21]–[23], but to date there is little research that addresses the case of plug-in HEVs [24]. As shown in [25], the performance of eco-routing algorithms is highly sensitive to the energy model used to estimate the energy cost on each link of the network. The challenging aspect of solving the eco-routing algorithm for plug-in HEVs relies on finding an energy model for these types of vehicles which can calculate both the electrical energy consumption and the fuel consumption. Jurik et al. [26] used the longitudinal dynamics to address the eco-routing problem for HEVs. A charge depleting first approach was studied in [27] and [28] to find the eco-route for plug-in HEVs. More recently, De Nunzio et al. proposed a semi-analytical solution of the powertrain energy management based on Pontryagin’s minimum principle to address the eco-routing of HEVs [29]. Houshmand et al. [30] devised a combined routing and powertrain control algorithm which simultaneously finds the energy optimal route as well as the optimal energy management strategy in terms of battery state of charge and fuel consumption. In [30], however, the possibility to recharge the battery on some parts of the route was neglected and only charge-sustaining or discharging operation was allowed.

Statement of Contributions: In this paper we devise optimal eco-routing strategies for plug-in HEVs by jointly optimizing the route and the high-level energy management strategy with objective of minimizing a combination of travel time and energy consumption. In particular, we first formulate the fuel-optimal energy management problem for a given driving cycle consisting of a predefined speed-trajectory to be followed. Considering a road network, we associate each road link with a predefined driving cycle capturing the road type and the traffic level. Using the PMP-based approach presented in [31], we rapidly solve the fuel-optimal energy management problem with a high-fidelity vehicle model for different battery charge targets and generate a Pareto front for each road link, describing the fuel consumption that would result from traversing it with a given battery charge target. Finally, we leverage the Pareto fronts to formulate the optimal eco-routing problem using a network flow model that can be parsed as a mixed-integer linear program (MILP) and solved with off-the-shelf optimization algorithms. This way, given an origin-destination pair and a desired battery state of energy at the end of the driving mission, our approach provides the optimal route to be followed together with an optimal battery energy trajectory that can be tracked by on-board energy management systems. We test our algorithm on the Eastern Massachusetts highway sub-network, showing that eco-routing strategies can significantly reduce fuel consumption and distance driven with merely limited increase in travel time.

This paper is structured as follows: In Section II we introduce the model of the PHEV and formulate the optimal eco-routing problem as a MILP. We present numerical results in Section III and conclude the paper in Section IV with a discussion and an overview on future research.

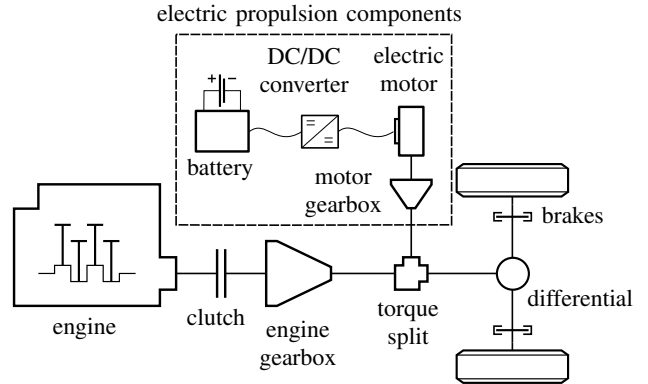


Fig. 2. P3 parallel-hybrid powertrain configuration.

II. METHODOLOGY

This section introduces a flow optimization approach for eco-routing. We first describe the model of the plug-in HEV in Section II-A. Second, we compute the Pareto fronts for fuel and battery energy for different driving cycles in Section II-B. Finally, Section II-D formulates the optimal routing and energy management problem for a given road network.

A. Plug-in Hybrid Electric Vehicle Model

Without loss of generality, we consider the P3 parallel-hybrid electric powertrain shown in Fig. 2 consisting of an ICE, a single-clutch gearbox, a single electric machine connected to a fixed-transmission-ratio gearbox and a battery. The modeling approach used in this work is based on [1]. For the sake of simplicity, we drop time-dependence whenever it is clear from the context.

Consider a driving cycle consisting of a speed trajectory $v(t)$, an acceleration trajectory $a(t)$ and a road grade trajectory $\vartheta(t)$. The required force at the wheels F_{req} results from the drag force F_d (comprising aerodynamic resistance, rolling friction and gravitational force) and the inertial force as

$$F_{\text{req}} = F_d(v, \vartheta) + m_{\text{tot}}(\gamma) \cdot a, \quad (1)$$

where ϑ is the road grade and m_{tot} accounts for the inertia of the vehicle and its moving parts as a function of the gear-ratio γ .

The speed and the torque at the torque-split result from the required force as a function of the wheel radius r_w and the final drive ratio γ_{fd} as

$$\omega_{\text{ts}} = v \cdot \frac{\gamma_{\text{fd}}}{r_w} \quad (2)$$

$$T_{\text{trac,ts}} = (F_{\text{req}} - F_{\text{brk}}) \cdot \frac{r_w}{\gamma_{\text{fd}}}, \quad (3)$$

where we assume the braking force F_{brk} to be positive only when the electric recuperation limit is reached. Given a motor torque at the torque-split $T_{\text{m,ts}}$, the resulting engine torque at the torque-split is

$$T_{\text{e,ts}} = T_{\text{trac,ts}} - T_{\text{m,ts}}. \quad (4)$$

We condense the clutch position and the selected gear in the variable i , with $i=0$ representing a disengaged clutch and the engine off, and $i>0$ an engaged clutch with a selected gear

$i \in \{1, 2, 3, 4, 5, 6\}$ and the engine on. The engine speed ω_e and the engine torque T_e result from the gearbox efficiency, the clutch position and the selected gear-ratio. If the clutch is engaged, the engine speed must be in the range

$$\omega_{e,\min} \leq \omega_e \leq \omega_{e,\max}, \quad (5)$$

whereas the maximum engine torque must be below a speed-dependent characteristic as

$$T_e \leq T_{e,\max}(\omega_e). \quad (6)$$

The fuel flow \dot{m}_f^* is given by the engine map

$$\dot{m}_f^* = \mathcal{M}_f(\omega_e, T_e). \quad (7)$$

The electrical power of the motor $P_{m,\text{el}}$ depends on its speed ω_m , torque T_m and efficiency η_m , which is characterized by the map

$$\eta_m = \mathcal{M}_m(\omega_m, T_m). \quad (8)$$

The minimum and maximum motor torques are given by the speed dependent characteristics

$$T_{m,\min}(\omega_m) \leq T_m \leq T_{m,\max}(\omega_m), \quad (9)$$

whereas the motor speed is limited as

$$0 \leq \omega_m \leq \omega_{m,\max}. \quad (10)$$

The power drawn at the battery terminal P_b is a sum of the electrical motor power and the power provided to the auxiliaries of the vehicle P_{aux} , i.e.,

$$P_b = P_{m,\text{el}} + P_{\text{aux}}. \quad (11)$$

Considering the DC-DC converter efficiency and the internal losses of the battery, the dynamics of the battery's state of energy are

$$\frac{d}{dt} E_b = -P_i, \quad (12)$$

where the internal battery power P_i is characterized by the map

$$P_i = \mathcal{M}_b(P_b, E_b). \quad (13)$$

Assuming a sufficiently large battery, we focus on the relative change in state of charge over the driving cycle given by

$$\Delta E_b(t) = E_b(t) - E_b(0). \quad (14)$$

This way we formulate the minimum-fuel control problem as follows.

Problem 1 (Minimum-fuel Energy Management Problem). *The optimal energy management strategy is found as the solution of*

$$\begin{aligned} & \min_{i, T_m} \int_0^T \dot{m}_f^*(t) dt \\ & \text{s.t. (1) – (14)} \\ & \Delta E_b(0) = 0 \\ & \Delta E_b(T) = \Delta E_{b,f}, \end{aligned} \quad (15)$$

where $\Delta E_{b,f}$ is the given charge or discharge target over the driving cycle.

The optimization problem 1 has one state variable (namely, ΔE_b) and two input variables (the clutch state with the

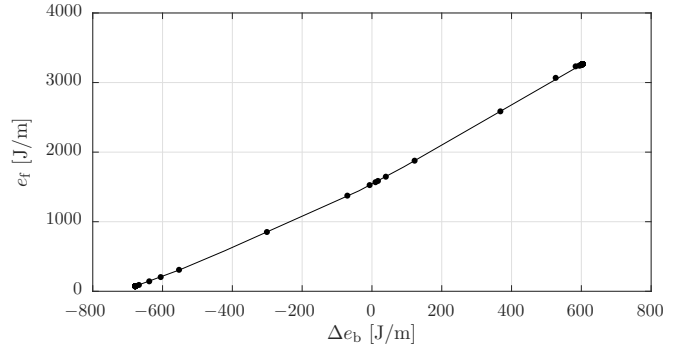


Fig. 3. Relative fuel energy consumption characteristic for a range of battery recharge targets (dots), and piecewise-affine fit (solid line).

selected gear i as well as the motor torque T_m). Therefore, it can be solved with optimization approaches such as dynamic programming. Alternatively, non-causal PMP can be used to simulate a perfectly tuned energy management system [31].

B. Pareto Frontiers

Given a driving cycle $v(t)$, $a(t)$, $\vartheta(t)$, we solve problem 1 for a set of $\Delta E_{b,f}$ and store its optimal objective as the corresponding fuel energy consumption:

$$E_f(\Delta E_{b,f}) = H_l \cdot \int_0^T \dot{m}_f^*(t) dt, \quad (16)$$

where $\dot{m}_f^*(t)$ is the solution to (15) given $\Delta E_{b,f}$, and H_l stands for the lower heating value of the fuel. Scaling the fuel and battery energy with the length of the driving cycle S , we obtain the discrete characteristic $e_f(\Delta e_b)$ shown in Fig. 3, where $e_f = E_f/S$ and $\Delta e_b = \Delta E_b/S$. Finally, we fit the Pareto front with the convex piecewise affine function

$$e_f(\Delta e_b) = a_k \cdot \Delta e_b + b_k \quad \text{if } \Delta e_b \in [\Delta e_b^k, \Delta e_b^{k+1}), \quad (17)$$

whereby $a_k \leq a_{k+1}$ and $a_k \cdot \Delta e_b^{k+1} + b_k = a_{k+1} \cdot \Delta e_b^{k+1} + b_{k+1}$, where $k \in [1, \dots, K] = \mathcal{K}$ and K is the number of affine lines. Moreover, we set the reachable battery discharge and charge limits as $\Delta e_{b,\min} = \Delta e_b^1$ and $\Delta e_{b,\max} = \Delta e_b^{K+1}$.

C. Road Digraph

We model the road network as a digraph $\mathcal{G} = (\mathcal{V}, \mathcal{A})$ consisting of a set of vertices \mathcal{V} and a set of arcs $\mathcal{A} \subseteq \mathcal{V} \times \mathcal{V}$. Herein, vertices $i \in \mathcal{V}$ represent intersections and arcs $(i, j) \in \mathcal{A}$ road links. Each arc has a specific length d_{ij} and a travel time t_{ij} , and is associated with a driving cycle representing the road type through the parameters $\{a_k(i, j), b_k(i, j)\}_k$ of the Pareto front presented in the previous Section II-B. This way, we capture fuel consumption as a function of battery energy consumption, assuming that fuel-optimal energy management strategies are used.

D. Eco-driving Problem Formulation

We capture the chosen route with the binary variable $x(\cdot, \cdot) \in \{0, 1\}^N$, which is 1 for each arc (i, j) traversed and 0 otherwise, and where $N = |\mathcal{A}|$ is the cardinality of the arc set. We define the fuel consumption to cross an arc on \mathcal{A} as $E_f(\cdot, \cdot) \in \mathbb{R}_+^N$ and the change in battery state of energy as $\Delta E_b(\cdot, \cdot) \in \mathbb{R}^N$. Given an origin $o \in \mathcal{V}$, a destination $d \in \mathcal{V}$,

an initial battery energy $E_{b,0}$, and a minimum and maximum battery energy $E_{b,min}$ and $E_{b,max}$, respectively, it holds that

$$\sum_{i:(i,j) \in \mathcal{A}} x(i,j) + \mathbb{1}_{j=o} = \sum_{k:(j,k) \in \mathcal{A}} x(j,k) + \mathbb{1}_{j=d} \quad \forall j \in \mathcal{V} \quad (18a)$$

$$x(i,j) \in \{0, 1\} \quad \forall (i,j) \in \mathcal{A} \quad (18b)$$

$$E_f(i,j) \geq 0 \quad \forall (i,j) \in \mathcal{A} \quad (18c)$$

$$E_{b,0} + \sum_{(i,j) \in \mathcal{A}} \Delta E_b(i,j) \in [E_{b,min}, E_{b,max}] \quad (18d)$$

$$\Delta E_b(i,j) \in [\Delta e_{b,min}(i,j), \Delta e_{b,max}(i,j)] \cdot d_{ij} \quad \forall (i,j) \in \mathcal{A}, \quad (18e)$$

where $\mathbb{1}_{\{\cdot\}}$ is a Boolean indicator function. Specifically, we preserve route continuity and integrality in (18a) and (18b). We allow fuel consumption to be non-negative in (18c), enforce the state of energy of the battery at the end of the mission to be within the battery size in (18d), and limit the reachable battery charge and discharge in (18e) depending on the arc length. We define the eco-routing objective as the monetarily weighted combination of travel time and fuel and battery consumption \square

$$J_1(x(\cdot, \cdot), E_f(\cdot, \cdot), \Delta E_b(\cdot, \cdot)) = \sum_{(i,j) \in \mathcal{A}} \left(\alpha \cdot V_t \cdot t_{ij} + (1 - \alpha) \cdot (V_f \cdot E_f(i,j) - V_e \cdot \Delta E_b(i,j)) \right) \cdot x(i,j), \quad (19)$$

where $\alpha \in (0, 1)$ is a time-to-energy weighting factor, whilst V_t, V_f, V_e represent the cost of time, fuel and electricity. We formally state the optimal eco-routing problem as follows.

Problem 2 (Eco-routing Problem). *The optimal eco-routing strategy is found as the solution of*

$$\min_{x(\cdot, \cdot), E_f(\cdot, \cdot), \Delta E_b(\cdot, \cdot)} J_1(x(\cdot, \cdot), E_f(\cdot, \cdot), \Delta E_b(\cdot, \cdot)) \quad (20a)$$

s.t. (18)

$$E_f(i,j) = \begin{cases} a_k(i,j) \cdot \Delta E_b(i,j) + b_k(i,j) \cdot d_{ij} & \text{if } x(i,j) = 1 \\ 0 & \text{if } x(i,j) = 0 \end{cases} \quad \forall k \in \mathcal{K}, (i,j) \in \mathcal{A} \quad (20b)$$

$$\Delta E_b(i,j) = 0 \quad \text{if } x(i,j) = 0 \quad \forall (i,j) \in \mathcal{A}, \quad (20c)$$

where $\{a_k(\cdot, \cdot)\}_k$ and $\{b_k(\cdot, \cdot)\}_k$ represent the Pareto optimal fuel-to-battery line for every road arc.

Problem 2 has a non-smooth and nonlinear form. However, it can be relaxed to a mixed-integer linear problem by first defining the cost

$$J_2(x(\cdot, \cdot), E_f(\cdot, \cdot), \Delta E_b(\cdot, \cdot)) = \sum_{(i,j) \in \mathcal{A}} \alpha \cdot V_t \cdot t_{ij} \cdot x(i,j) + (1 - \alpha) \cdot (V_f \cdot E_f(i,j) - V_e \cdot \Delta E_b(i,j)), \quad (21)$$

and then stating the relaxed eco-routing problem using the big-M formulation as follows [32].

Problem 3 (Relaxed Eco-routing Problem). *The relaxed optimal eco-routing problem is*

$$\min_{x(\cdot, \cdot), E_f(\cdot, \cdot), \Delta E_b(\cdot, \cdot)} J_2(x(\cdot, \cdot), E_f(\cdot, \cdot), \Delta E_b(\cdot, \cdot)) \quad (22a)$$

s.t. (18)

$$E_f(i,j) \geq a_k(i,j) \cdot \Delta E_b(i,j) + b_k(i,j) \cdot d_{ij} - M \cdot (1 - x(i,j)) \quad \forall k \in \mathcal{K}, (i,j) \in \mathcal{A} \quad (22b)$$

$$\Delta E_b(i,j) \in [-1, 1] \cdot M \cdot x(i,j) \quad \forall (i,j) \in \mathcal{A}, \quad (22c)$$

where M is a sufficiently large number.

This problem can be solved using off-the-shelf mixed-integer linear program solvers. In the following lemma, we prove that the solution to both problems is equivalent.

Lemma II.1 (Problem Equivalence). *The solution of Problem 3 is also the solution of Problem 2.*

Proof. Given M sufficiently large, constraint (22c) is equivalent to (20c). Similarly, constraint (22b) is the convex relaxation of (20b). Moreover, by inspection we see that the minimizer of (22a) is a minimizer of (20a). We conclude the rest of the proof by contradiction. Assume that the solution of Problem 3 is not a feasible solution of Problem 2. This means that constraints (18c) and (22b) hold with inequality on some arc $(i,j) \in \mathcal{A}$. Therefore, one could find a solution with a smaller $E_f(i,j)$ such that either (18c) (if $x(i,j) = 0$) or (22b) (if $x(i,j) = 1$) hold with equality. Due to objective (22a), this means that the solution of Problem 3 is not optimal, contradicting the initial assumption. Therefore, the solution of Problem 3 is also the solution of Problem 2, which concludes the proof. \square

E. Discussion

A few comments are in order. First, we focus on a P3 hybrid electric powertrain architecture. Nevertheless, the proposed methodology can be applied to any hybrid powertrain topology with a power-split device. Second, the proposed approach does not allow including the battery size in the form of a path constraint, but it can be included as a terminal constraint. Such an assumption is in order for large batteries (as is the case for plug-in HEVs) and little elevation difference. To include path constraints, one should know the order of the arcs in the path within the optimization problem, which is not possible in the current formulation. One possibility could be to expand the graph in layers describing the state of charge of the battery, as done in [33].

III. RESULTS

In order to evaluate the performance of the proposed algorithm, we conduct a data-driven case study using the actual traffic data from the Eastern Massachusetts (EMA) road network collected by INRIX [34]. The sub-network including the interstate highways of EMA (Fig. 4 left) is chosen for the case study. Each link consists of several arcs referred to as *traffic message channels* in the dataset. In this sub-network, we have 298 road segments (considering both directions on each road), and the average speed of each segment is available for the entire year of 2012 on a minute-by-minute basis. Details regarding this sub-network can be found in [34]. As an alternative benchmark, the traffic behaviour of the network has been simulated in SUMO [35] using the extracted flow data from the aforementioned traffic data-set. We consider two sub-networks of the EMA traffic network to apply our algorithms: the EMA small sub-network shown in Fig. 4 left and the EMA medium sub-network shown in Fig. 4 right. Since the Boston area does not display significant elevation changes, we classify each link of the road graph as a function of the traffic speed and associate them with the urban, the suburban and the highway driving cycles NYC, UDDS and HWFET, respectively [36] (Table I). We consider a full-size plug-in HEV with a gasoline ICE and a 20 MJ battery

TABLE I
DRIVING CYCLE ASSIGNMENT FOR EACH ROAD LINK

Traffic Mode	Average speed on the Link (kmph)	Driving Cycle
Heavy Traffic	[0,32]	NYC
Medium Traffic	(32,64]	UDDS
Low Traffic	> 64	HWFET

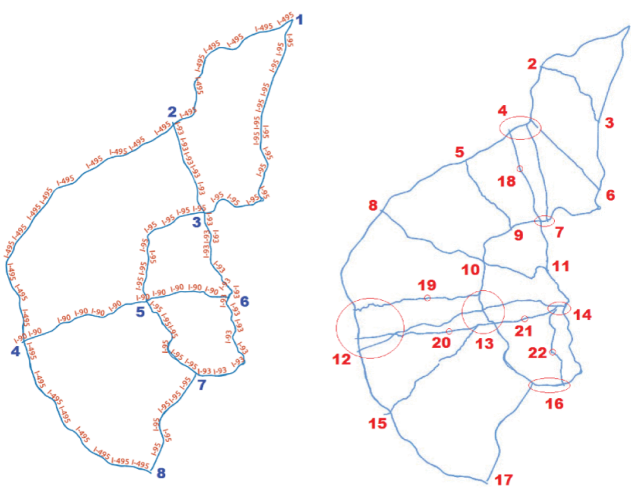


Fig. 4. EMA small sub-network (left) and EMA medium sub-network (right) [34].

and compute the Pareto front for each of the driving cycles with [31]. Fig. 3 shows the results for the HWFET driving cycle. Each Pareto front was computed in about 5 s. Finally, we set the value of time V_t to 24.40 USD/h [37], whilst the cost of gasoline V_f and electricity V_e are set equal to 2.75 USD/gal (i.e., 0.023 USD/MJ) [38] and 0.114 USD/kWh (i.e., 0.032 USD/MJ) [39], respectively.

A. Small Eastern Massachusetts Sub-network

Initially we assess the performance of the proposed eco-routing algorithm by finding energy optimal routes over the small EMA sub-network shown in Fig. 4 left. To conduct a data-driven case study, we use the actual traffic data from the Eastern Massachusetts (EMA) road network. These data were collected by INRIX and provided by the Boston Region Metropolitan Planning Organization, which includes average speed of every link on a minute-by-minute basis for 2012. To show the dependency of the eco-route on the speed of links, we calculate the eco-route for different times of April 12, 2012, and show the energy cost and travel time for travelling between node 1 and 5 (see Fig. 4 left). We compute the optimal route for different hours of that day. This way, we analyse the effect of traffic on the solution. Moreover, to investigate the effect of the time-to-energy weight α on the optimal routes and their corresponding cost and time, we solve Problem 3 for α equal to almost 0, almost 1 (since with α equal exactly 0 or 1, Problem 3 would relax) and 0.5, corresponding to the time-optimal route, the energy-optimal eco-route and the cost-optimal route (where the monetary values of time, fuel and electricity are used as weights), respectively. The solution of each problem took about 200 ms

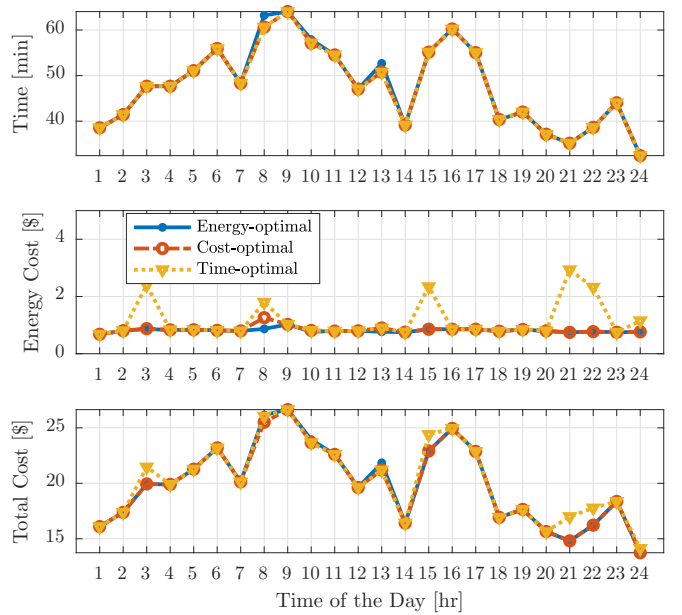


Fig. 5. Travel time, energy cost, and total cost for the O-D pair (1,5) in the EMA small sub-network.

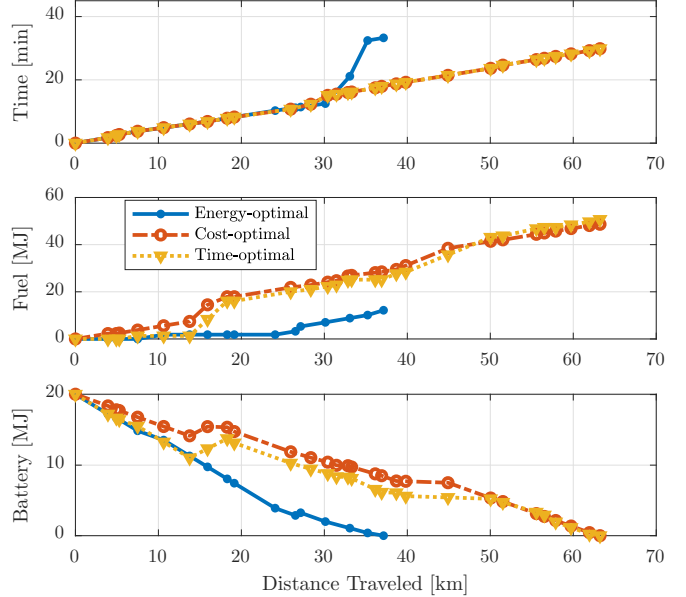


Fig. 6. Travel time, fuel consumption and battery state of energy along the optimal routes for the O-D pair (2,7) in the medium EMA sub-network.

using Gurobi 8.1 [40] on commodity hardware. The results for the O-D pair (1,5) in the EMA small sub-network shown in Fig. 5 reveal that sometimes energy consumption can be significantly reduced at the expense of little extra travel time.

B. Medium Eastern Massachusetts Sub-network with Traffic Simulation

Since we did not want to rely solely upon the historical traffic data to validate our routing algorithm, we decided to simulate the traffic of the medium EMA sub-network shown in Fig. 4 right, using SUMO (Simulation of Urban MObility) [35]. Herein, we used the INRIX data to start the simulation in SUMO to extract the flow data for the

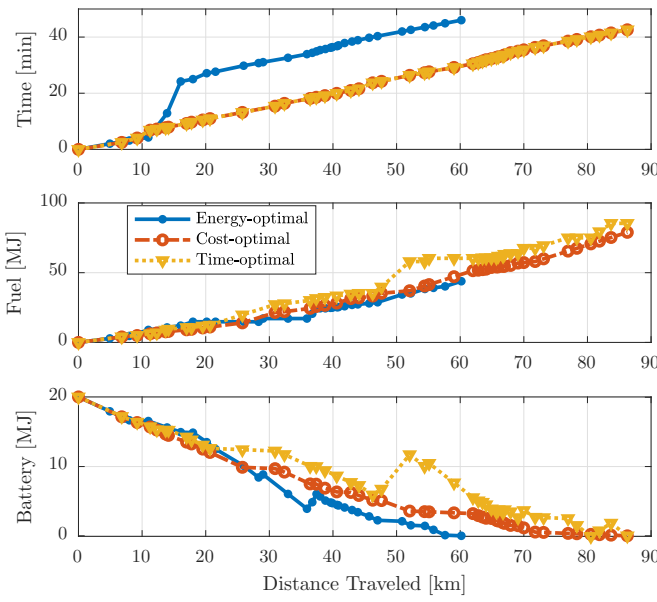


Fig. 7. Travel time, fuel consumption and battery state of energy along the optimal routes for the O-D pair (4,16) in the medium EMA sub-network.

sub-network. The details of these calculations can be found in [34], [41].

We then aggregated every 5 segments in the map into a single arc and recorded its average speed. Thus we ended up with a road graph consisting of 694 nodes and 617 arcs. Similarly as in the previous Section III-A, we compute the optimal route and battery usage minimizing travel time, cost and energy consumption for each of these routes for different O-D pairs by solving Problem 3. The solution of each problem took about 200 ms using Gurobi 8.1 [40] on commodity hardware. Fig. 6 and 7 shows the cumulative travel time, fuel consumption and battery state of energy for the O-D pairs (2,7) and (4,16), respectively. Given the plug-in nature of the HEV, the battery is always discharged. For both O-D pairs, the time-optimal solution (yellow) entails the highest fuel consumption. The cost-optimal (red) achieves the same performance, whilst saving fuel due to the energy-optimal energy management. The eco-route (blue), being significantly shorter and slower, saves more than 50% in terms of fuel consumption at the expense of about 10% travel time. Fig. 8 shows the achieved travel time and fuel consumption for different values of α , whereby the non-smooth shape of the plot results from the discrete nature of the routing problem, and highlights the fact that by sacrificing a minor amount of travel time, fuel consumption can be significantly reduced by taking a shorter and slower route.

IV. CONCLUSION

This paper presented an eco-routing algorithm to jointly compute the optimal route and energy management strategy for plug-in hybrid electric vehicles. Specifically, we first parametrized the achievable fuel consumption as a function of battery usage for different driving cycles, which we used to characterize the road arcs in the network. Second, we used a flow optimization model to formulate the optimal eco-routing problem as a mixed-integer linear program that could

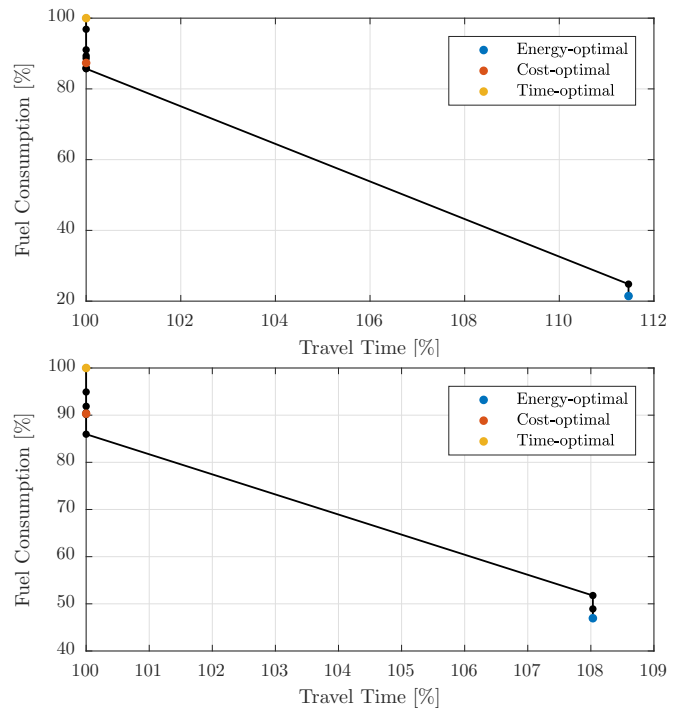


Fig. 8. Relative fuel consumption and travel time for O-D pair (2,7) (upper plot) and (4,16) (lower plot) for different values of $\alpha \in (0, 1)$.

be rapidly solved with off-the-shelf optimization algorithms. Finally, we validated the proposed algorithm on the Eastern Massachusetts highway sub-network. Our results showed that our approach can rapidly compute the optimal route and energy management strategy for different optimization objectives, and revealed that fuel consumption can be significantly reduced at the expense of very little travel time.

This work can be extended in several directions. On the one hand, we would like to explicitly include path constraints such as battery size, for instance by expanding the graph to capture different battery charge levels, as proposed in [33]. On the other hand, it is of interest to extend such an approach to large fleets of vehicles providing on-demand mobility [42]–[45].

ACKNOWLEDGMENTS

We would like to express our gratitude to Dr. I. New, Mr. J. Ritzmann, Mr. A. Christon, Mr. N. Lanzetti and Mr. P. Duhr for their assistance with the proofreading, useful advice and comments. The first author thanks Prof. Ch. Onder for his support. This research was supported by the National Science Foundation under CAREER Award CMMI-1454737 and the Toyota Research Institute (TRI). This work was also supported in part by NSF under grants ECCS-1509084, DMS-1664644, CNS-1645681, by AFOSR under grant FA9550-19-1-0158, by ARPA-E's NEXTCAR program under grant DE-AR0000796 and by the MathWorks. This article solely reflects the opinions and conclusions of its authors and not NSF, TRI, or any other entity.

REFERENCES

[1] L. Guzzella and A. Sciarretta, *Vehicle Propulsion Systems*. Springer Berlin Heidelberg, 2007.

[2] D. V. Collia, J. Sharp, and L. Giesbrecht, "The 2001 national household travel survey: A look into the travel patterns of older Americans," *Journal of safety research*, vol. 34, no. 4, pp. 461–470, 2003.

[3] L. V. Pérez and E. A. Pilotta, "Optimal power split in a hybrid electric vehicle using direct transcription of an optimal control problem," *Mathematics and Computers in Simulation*, vol. 79, no. 6, pp. 1959–1970, 2009.

[4] P. Elbert, S. Ebbesen, and L. Guzzella, "Implementation of dynamic programming for n -dimensional optimal control problems with final state constraints," *IEEE Transactions on Control Systems Technology*, vol. 21, no. 3, pp. 924–931, 2013.

[5] P. Elbert, T. Nüesch, A. Ritter, N. Murgovski, and L. Guzzella, "Engine on/off control for the energy management of a serial hybrid electric bus via convex optimization," *IEEE Transactions on Vehicular Technology*, vol. 63, no. 8, pp. 3549–3559, 2014.

[6] S. Ebbesen, M. Salazar, P. Elbert, C. Bussi, and C. H. Onder, "Time-optimal control strategies for a hybrid electric race car," *IEEE Transactions on Control Systems Technology*, vol. 26, no. 1, pp. 233–247, 2018.

[7] N. Robuschi, M. Salazar, P. Duhr, F. Braghin, and C. H. Onder, "Minimum-fuel engine on/off control for the energy management of hybrid electric vehicles via iterative linear programming," in *IFAC Symposium on Advances in Automotive Control (AAC)*, 2019.

[8] A. Sciarretta and L. Guzzella, "Control of hybrid electric vehicles," *Control systems, IEEE*, vol. 27, no. 2, pp. 60–70, 2007.

[9] A. Sciarretta, G. De Nunzio, and L. L. Ojeda, "Optimal ecodriving control: Energy-efficient driving of road vehicles as an optimal control problem," *Control Systems, IEEE*, vol. 35, no. 5, pp. 71–90, 2015.

[10] M. Salazar, P. Elbert, S. Ebbesen, C. Bussi, and C. H. Onder, "Time-optimal control policy for a hybrid electric race car," *IEEE Transactions on Control Systems Technology*, vol. 25, no. 6, pp. 1921–1934, 2017.

[11] L. Guzzella and A. Sciarretta, *Vehicle propulsion systems*, 3rd ed. Berlin: Springer, 2013.

[12] T. Hofman, M. Steinbuch, R. Van Druten, and A. Serrarens, "Rule-based energy management strategies for hybrid vehicles," *International Journal of Electric and Hybrid Vehicles*, vol. 1, no. 1, pp. 71–94, 2007.

[13] T. Nüesch, A. Cerfolini, G. Mancini, N. Cavina, C. Onder, and L. Guzzella, "Equivalent consumption minimization strategy for the control of real driving nox emissions of a diesel hybrid electric vehicle," *Energies*, vol. 7, no. 5, pp. 3148–3178, 2014.

[14] M. Salazar, C. Balerna, E. Chisari, C. Bussi, and C. H. Onder, "Equivalent lap time minimization strategies for a hybrid electric race car," accepted for *IEEE Control and Decision Conference*, 2018.

[15] H. Borhan, A. Vahidi, A. M. Phillips, M. L. Kuang, I. V. Kolmanovsky, and S. Di Cairano, "MPC-based energy management of a power-split hybrid electric vehicle," *IEEE Transactions on Control Systems Technology*, vol. 20, no. 3, pp. 593–603, 2012.

[16] L. Johannesson, N. Murgovski, E. Jonasson, J. Hellgren, and B. Egardt, "Predictive energy management of hybrid long-haul trucks," *Control Engineering Practice*, vol. 41, pp. 83–97, 2015.

[17] M. Salazar, C. Balerna, P. Elbert, F. P. Grando, and C. H. Onder, "Real-time control algorithms for a hybrid electric race car using a two-level model predictive control scheme," *IEEE Transactions on Vehicular Technology*, vol. 66, no. 12, pp. 10911–10922, 2017.

[18] D. Ambühl and L. Guzzella, "Predictive reference signal generator for hybrid electric vehicles," *IEEE Transactions on Vehicular Technology*, vol. 58, no. 9, pp. 4730–4740, 2009.

[19] D. P. Bertsekas, *Dynamic programming and optimal control*. Athena scientific, Belmont, MA, 1995, vol. 1, no. 2.

[20] K. Braekers, K. Ramaekers, and I. Van Nieuwenhuyse, "The vehicle routing problem: State of the art classification and review," *Computers & Industrial Engineering*, vol. 99, pp. 300–313, Sept. 2016. [Online]. Available: <http://linkinghub.elsevier.com/retrieve/pii/S0360835215004775>

[21] M. Barth, K. Boriboonsomsin, and A. Vu, "Environmentally-friendly navigation," in *Intelligent Transportation Systems Conference, 2007. ITSC 2007. IEEE*. IEEE, 2007, pp. 684–689.

[22] O. Andersen, C. S. Jensen, K. Torp, and B. Yang, "EcoTour: Reducing the Environmental Footprint of Vehicles Using Eco-routes," in *2013 IEEE 14th International Conference on Mobile Data Management*, vol. 1, June 2013, pp. 338–340.

[23] B. Yang, C. Guo, C. S. Jensen, M. Kaul, and S. Shang, "Stochastic skyline route planning under time-varying uncertainty," in *2014 IEEE 30th International Conference on Data Engineering*, Mar. 2014, pp. 136–147.

[24] J. Guanetti, Y. Kim, and F. Borrelli, "Control of connected and automated vehicles: State of the art and future challenges," *Annual Reviews in Control*, vol. 45, pp. 18–40, Jan. 2018. [Online]. Available: <http://www.sciencedirect.com/science/article/pii/S1367578818300336>

[25] M. Kubička, J. Klusáček, A. Sciarretta, A. Cela, H. Mounier, L. Thibault, and S.-I. Niculescu, "Performance of current eco-routing methods," in *Intelligent Vehicles Symposium (IV), 2016 IEEE*. IEEE, 2016, pp. 472–477.

[26] A. Cela, T. Jurik, R. Hamouche, R. Natowicz, A. Reama, S. I. Niculescu, and J. Julien, "Energy Optimal Real-Time Navigation System," *IEEE Intelligent Transportation Systems Magazine*, vol. 6, no. 3, pp. 66–79, 2014.

[27] Z. Sun and X. Zhou, "To save money or to save time: Intelligent routing design for plug-in hybrid electric vehicle," *Transportation Research Part D: Transport and Environment*, vol. 43, pp. 238–250, Mar. 2016. [Online]. Available: <http://www.sciencedirect.com/science/article/pii/S1361920916000031>

[28] Z. Qiao and O. Karabasoglu, "Vehicle Powertrain Connected Route Optimization for Conventional, Hybrid and Plug-in Electric Vehicles," *arXiv:1612.01243 [cs]*, Dec. 2016, arXiv: 1612.01243. [Online]. Available: <http://arxiv.org/abs/1612.01243>

[29] G. D. Nunzio, A. Sciarretta, I. B. Gharbia, and L. L. Ojeda, "A Constrained Eco-Routing Strategy for Hybrid Electric Vehicles Based on Semi-Analytical Energy Management," in *2018 21st International Conference on Intelligent Transportation Systems (ITSC)*, Nov. 2018, pp. 355–361.

[30] A. Houshmand and C. G. Cassandras, "Eco-Routing of Plug-In Hybrid Electric Vehicles in Transportation Networks," in *2018 21st International Conference on Intelligent Transportation Systems (ITSC)*. IEEE, 2018, pp. 1508–1513.

[31] J. Ritzmann, A. Christon, M. Salazar, and C. H. Onder, "Fuel-optimal power split and gear selection strategies for a hybrid electric vehicle," in *SAE International Conference on Engines & Vehicles*, 2019.

[32] A. Richards and J. How, "Mixed-integer programming for control," in *American Control Conference*, 2005.

[33] F. Rossi, R. Iglesias, M. Alizadeh, and M. Pavone. (2017) On the interaction between autonomous mobility-on-demand systems and the power network: models and coordination algorithms. Extended version Available at <http://arxiv.org/abs/1709.04906>.

[34] J. Zhang, S. Pourazarm, C. G. Cassandras, and I. C. Paschalidis, "The price of anarchy in transportation networks: Data-driven evaluation and reduction strategies," *Proceedings of the IEEE*, 2018.

[35] D. Krajzewicz, J. Erdmann, M. Behrisch, and L. Bieker, "Recent development and applications of SUMO-Simulation of Urban MObility," *International Journal On Advances in Systems and Measurements*, vol. 5, no. 3&4, 2012.

[36] (2018) Nrel drivecat - chassis dynamometer drive cycles - new york city cycle. National Renewable Energy Laboratory. Available online. [Online]. Available: <http://www.nrel.gov/transportation/drive-cycle-tool>

[37] U.S. Dept. of Transportation, "Revised departmental guidance on valuation of travel time in economic analysis," Tech. Rep., 2015.

[38] "Energy Information Administration - The U.S. Weekly Retail Gasoline and Diesel Prices. U.S. Department of Energy." 2019.

[39] "Energy Information Administration - Average Retail Price of Electricity to Ultimate Customers: Total by End-Use Sector. U.S. Department of Energy." 2019.

[40] L. Gurobi Optimization, "Gurobi optimizer reference manual," 2018. [Online]. Available: <http://www.gurobi.com>

[41] S. Pourazarm, C. G. Cassandras, and T. Wang, "Optimal routing and charging of energy-limited vehicles in traffic networks," *Int. J. Robust. Nonlinear Control*, vol. 26, no. 6, pp. 1325–1350, Apr. 2016. [Online]. Available: <http://onlinelibrary.wiley.com/doi/10.1002/rnc.3409/abstract>

[42] M. Salazar, F. Rossi, M. Schiffer, C. H. Onder, and M. Pavone, "On the interaction between autonomous mobility-on-demand and the public transportation systems," in *Proc. IEEE Int. Conf. on Intelligent Transportation Systems*, 2018, Extended Version, Available at <https://arxiv.org/abs/1804.11278>.

[43] M. Tsao, D. Milojevic, C. Ruch, M. Salazar, E. Frazzoli, and M. Pavone, "Model predictive control of ride-sharing autonomous mobility on demand systems," in *Proc. IEEE Conf. on Robotics and Automation*, 2019, in Press.

[44] M. Salazar, N. Lanzetti, F. Rossi, M. Schiffer, and M. Pavone, "Intermodal autonomous mobility-on-demand," *IEEE Transactions on Intelligent Transportation Systems*, 2019, submitted.

[45] M. Salazar, M. Tsao, I. Aguiar, M. Schiffer, and M. Pavone, "A congestion-aware routing scheme for autonomous mobility-on-demand systems," in *European Control Conference*, 2019, in Press.